



Time domain reflectometry sensor-assisted freeze/thaw analysis in geomaterials

Zhen Liu, Xiong (Bill) Yu^{*}, Xinbao Yu, Javanni Gonzalez

ARTICLE INFO

Article history:

Received 20 March 2011

Accepted 9 October 2011

Keywords:

Freeze/thaw effects
Sensor assisted analysis
TDR tube sensor
Geomaterials

ABSTRACT

Freeze–thaw is a major source of damages and deteriorations for infrastructures in cold regions. Most of the existing investigations focus on soil behaviours in the completely frozen or completely thawed state. Tools to assist the determination of freeze/thaw status and its effects on geomaterials including soils are currently rare. This paper firstly introduced the design of an innovative guided electromagnetic wave sensor called Time Domain Reflectometry (TDR) tube that can non-destructively monitor the freeze/thaw process in standard sized soil specimens. An analysis algorithm was presented for interpreting TDR signals accordingly to determine the degree of freeze/thaw. The determined freeze/thaw statuses were then compared with deformation moduli obtained with compression test. An empirical relationship for freeze–thaw status-dependent mechanical properties was proposed based on the experimental observation. On the other hand, a framework of sensor-assisted analysis of freeze/thaw effects on soils was established. The framework concentrates on mechanical behaviours including stresses and deformations which are responsible for the distresses in the infrastructures. Poroelastic relationships, macro–micro relationship and the thermal dynamic equilibriums between phases were incorporated to obtain a close form solution for the simulation model. A simple case study was conducted to demonstrate the fusion of sensor data and computational simulation to investigate the freeze/thaw effects on soils.

© 2011 Elsevier B.V. All rights reserved.

1. Introduction

Freeze–thaw cycle associated with frost heaving or strength loss may cause extensive damages to various civil-engineering structures, such as pavement and utility lines. For example, the ice enrichment in pavement foundations can lead to serious problems, i.e., an uneven uplift during freezing and then a loss of support when ice lenses thaw (Konrad, 1994). It thus easily threatens the serviceability and sustainability of these structures and consequently increases their cost of construction and maintenance.

While extensive studies have been conducted on frozen soils, our current knowledge on soil behaviours during freeze–thaw process is still limited. Firstly, several attempts have been made to quantify the effects of freeze/thaw experimentally. A typical quantity, i.e., degree of freezing/thawing, has been frequently adopted and measured. However, there exist different limitations in these commonly used technologies for frost measurements (Yu et al., 2010). For example, frost tubes (plastic fluorescent dye tubes), which undergo a color change as a result of a freezing/thawing process, do not measure the extent of freezing/thawing development (Frost Resistivity Probe User Guide, 1996; Roberson and Siekmeier, 2000). Resistivity Probes, which measure the electrical resistance of soils, require subjective data analysis and have to be supplemented with thermocouple data (Klut, 1986; Roberson and Siekmeier, 2000). Innovative design of experimental tool is necessary for further investigating soil behaviours during freezing/thawing process.

On the other hand, there have been efforts in theoretical modeling the freeze/thaw effects on soils (Neaupane and Yamabe, 2001; Nishimura et al., 2009). These models usually employed a thermo-hydro-mechanical field to allow for the mechanical responses resulting from subfreezing boundary conditions. However, these models are inevitably attended with high nonlinearity due to the complex coupling effects. Consequently, the dependence on initial and boundary conditions and materials properties hampered the application of these models.

In this paper, a TDR sensor-assisted freeze/thaw analysis approach for soil is presented. It is the first time the TDR sensor technology is proposed to assist the freeze/thaw analysis with a theoretical mechanical model. The main contribution to the frost engineering community and sensor research community is three folded: 1) TDR sensor as a tool in freeze/thaw analyses is explored and tested with the assistance of conventional Civil Engineering experiments; 2) the concept of sensor-assisted analysis is realized with a proposed theoretical framework based on continuum mechanics, thermal dynamics and macro–micro relationships and etc. In another word, the real-time monitoring with a TDR sensor is combined with theoretical formulation to bridge the gap between simulations and real-time sensor monitoring data; 3) the potential application of this technique is demonstrated with a simplified model in a case study.

2. Theory of TDR instrument in freezing soils

The Time Domain Reflectometry (TDR) is a guided radar technology. It measures the responses of materials under the excitation of a fast rising electric pulse. Information directly obtained is material electrical properties such as the apparent dielectric constant and the electrical conductivity. The former is related to the speed of electromagnetic wave in the

^{*} Corresponding author at: 2104 Adelbert Road, Bingham 206, Cleveland, Ohio 44106, USA, Tel.: +1 216 368 6247.

E-mail address: xxy21@case.edu (X.(B.) Yu).

material while the latter is related to the energy attenuation. Both quantities can be easily obtained from one TDR signal (Klut, 1986; Topp et al., 1980).

The travelling velocity of an electromagnetic wave in a medium, v , can be calculated as follows:

$$v = \frac{c}{\sqrt{K_a}} \quad (1)$$

where c is the velocity of an electromagnetic wave in a vacuum (2.988×10^8 m/s) and K_a is the dielectric constant. This quantity is generally referred to as the apparent dielectric constant for TDR measurement in soils. The time for the electromagnetic wave travelling down and back along a metallic waveguide of length, L , is given by:

$$t = \frac{2L}{v} \quad (2)$$

Substituting Eqs. (1) to (2) yields

$$K_a = \left(\frac{ct}{2L}\right)^2 \quad (3)$$

By defining $ct/2$ as the apparent length, L_a , the apparent dielectric constant can be calculated as:

$$K_a = \left(\frac{L_a}{L}\right)^2 \quad (4)$$

In a TDR signal, the apparent length is determined by analyzing the elapsed time between reflections (in Fig. 1). The electrical conductivity of bulk soil sample can be simultaneously obtained from the final signal level (Yu and Drnevich, 2004).

Water has a dielectric constant around 81, which is much larger than that of soil solids (typically around 3 to 7) or air (around 1). The dielectric constant of ice is approximately equal to those of solids. The significant change of dielectric constant between water in liquid or solid status makes it possible for TDR to measure the freezing process or vice versa.

The following concepts (Eqs. 5 and 6) were introduced to characterize the degree of freeze/thaw directly from TDR measurements.

$$\Phi = \frac{w_u - w_t}{w_u - w_f} \times 100\% \quad (5)$$

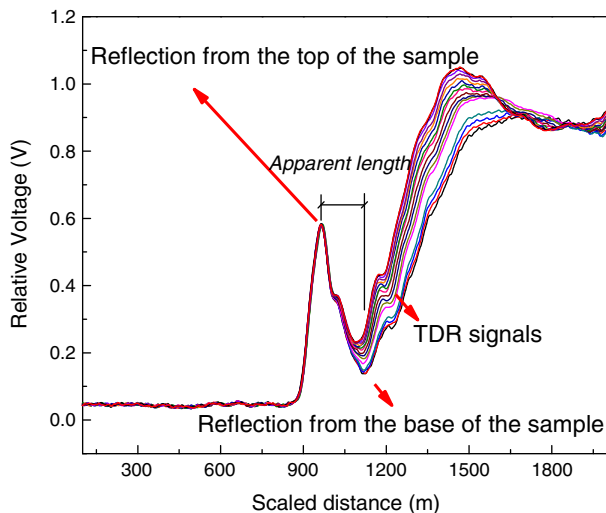


Fig. 1. Typical TDR signals and critical information.

where Φ is the degree of freeze, w_u is the gravimetric water content in a completely unfrozen state which is 100%; w_t is the gravimetric water content at time t of a freeze–thaw sample; w_f is the gravimetric water content in completely frozen samples. Since the state of 100% frozen is difficult to approach in reality, the water content at temperatures which are adequately lower than freezing point can be assumed to be w_f .

Siddiqui (Topp et al., 1980) developed an equation that relates TDR measured dielectric constant to gravimetric water content (gravimetric water content w , i.e., mass of water compared to mass of dry soil solids; volumetric water content, θ , i.e., volume of water compared to total volume of soil) (Drnevich et al., 2001; Siddiqui and Drnevich, 1995). This equation accounts for the effects of soil type and soil density by incorporating two calibration constants as the following.

$$w = \frac{1}{B} \left[\frac{\rho_w}{\rho_d} \sqrt{K_a} - A \right] \quad (6)$$

where ρ_w is the density of water, ρ_d is the dry density of soil, A and B are soil-dependent calibration constants, typically A is 1, and B is 8.

Substitute Eq. 6 to Eq. 5, there is (Siddiqui and Drnevich, 1995),

$$\Phi = \frac{\sqrt{K_{a,u}} - \sqrt{K_{a,t}}}{\sqrt{K_{a,u}} - \sqrt{K_{a,f}}} \times 100\% \quad (7)$$

where $K_{a,u}$ is the dielectric constant in the unfrozen sample, $K_{a,t}$ is the dielectric constant at time t of a freeze–thaw sample, $K_{a,f}$ is the dielectric constant in a completely frozen sample. Finally, by substituting Eq. 4 into Eq. 7, we obtain,

$$\Phi = \frac{L_{a,u} - L_{a,t}}{L_{a,u} - L_{a,f}} \times 100\% \quad (8)$$

Similarly, the concept of percent of thaw was defined and derived as Eq. 9,

$$\Sigma = \frac{L_{a,t} - L_{a,f}}{L_{a,th} - L_{a,f}} \times 100\% \quad (9)$$

where $L_{a,th}$ is the apparent length corresponding to the completely thawed state. During the freeze–thaw cycle, the degree of freezing and the degree of thawing are related by Eq. 10:

$$\Phi + \Sigma = 1 \quad (10)$$

The degree of freeze/thaw can readily be determined from TDR measured dielectric constant by the concept defined above.

3. Design and analysis of a TDR sensor

A TDR tube sensor was designed and fabricated to apply the above theory to the free/thaw status identification in soils. The outer shell of the sensor was made of Poly Vinyl Chloride. This material was chosen based on its high strength, small dielectric constant and smaller coefficient of thermal expansion. Hence the pipe is able to function as the main structure to hold the electrodes and accommodate the soil specimen without interrupting the electrostatic field. As shown in Fig. 2a, the pipe was designed as 4 mm thick and 100 mm high with an inner diameter of 35 mm. Two sheets of 0.09 mm-thick copper foils of the same height were deployed symmetrically on the inner surface of the pipe (green dashed area). Two surfaces passing the two adjacent edges of the copper foil and the axis of the pipe form an angle of 20° . For the whole TDR system, the sensor tube was connected to a TDR pulse generator by a coaxial cable. Delicate treatment was executed to eliminate the imperfections in the joints for the purpose of avoiding possible noise in the TDR signals.

Experiments were conducted on soil specimens prepared with a Harvard miniature compactor. Soil specimens can be non-intrusively monitored as the specimens were subjected to freezing/thawing conditions (Fig. 2b). There was no physical contact between soil specimen and the tube sensor throughout the experiments. More details can be found in the next section.

The validity of the sensor design was testified by a sensitivity analysis prior to the implementation. We know that TDR obtain results based on an energy-weighted algorithm. Hence the energy distribution around the tube sensor was obtained and analyzed firstly. It has been found that the energy was mostly distributed within the tube. Furthermore, the energy intensity was comparatively higher at neighbouring locations of electrodes. The validity of the design was therefore supported by this sensitivity analysis (Fig. 3).

Preliminary experiments were carried out with the self-developed tube sensor to test the above theory. Fig. 4 illustrates that the TDR sensor monitored the dielectric constant of a soil sample during a freeze–thaw cycle. Also plotted in Fig. 4 is the measured evolution of the electrical conductivity (inverse of resistivity). As shown in these figures, different stages of freeze/thaw can be clearly identified from the evolution curve of the measured dielectric constant. The change of dielectric constant is attributed to the change in the unfrozen water content.

4. Freeze–thaw status and soil mechanical properties

The degrees of thawing and mechanical properties during the thawing process were measured with the tube sensor. At the same time, conventional compression tests were conducted. The soil studied was sampled from MnRoad subgrade materials. It was a clay with low plasticity. The soil was first mixed with lime sludge powder at a ratio of 10:1. Water was then added to prepare specimens at water content of 12% and 15% respectively. Cylindrical specimens with a diameter of 34 mm and a height of 71 mm were prepared with a Harvard miniature compactor. A standard process was strictly followed to ensure the quality and similarity of these specimens; the total weight and water content were used as the control criteria. Subsequently, the specimens were installed in a freezer until they were completely frozen. These specimens were then taken out and exposed to the room temperature (22°C) to allow thawing to occur. The degree of thawing was independently measured by using the self-developed tube sensor. Monitored thawing status was compared with the temperature at the center of the specimen. As

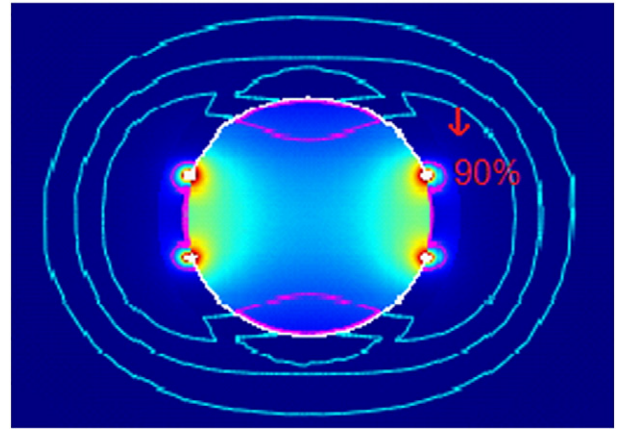


Fig. 3. Sensitivity analysis (energy distribution).

shown in Fig. 5, the degree of thawing increased as the temperature went up. And they match well at the time when the thawing process stopped. The comparison does not only validate the new method but also help in identifying the end of thaw or the beginning of freeze.

This method was then used in conjunction with a conventional experimental program to study the soil behaviours during freezing/thawing process. Typical results of practical interest, i.e., modulus and strength were investigated.

Fig. 6a illustrates that the axis strain varies with the vertical axial stress in the unconfined compression test. The peak strength and initial tangent moduli obtained from the stress–strain curves are shown in Fig. 6b. The moduli of specimens corresponding to different degrees of thawing were clearly shown to be significantly influenced by the amount of ice for either the maximum modulus or the peak strength value. The relationship between the maximum tangent modulus and the degree of thawing can be fitted well by a proposed function as follows,

$$E_t = C \cdot D^x \quad (11)$$

where E_t is the maximum tangent modulus, C, D are constants for curve fitting. For the specimen of water content 11.2% and 14.3% (measured after the experiments), the values of C/D are 13.5/0.915 and 21.57/0.93, respectively.

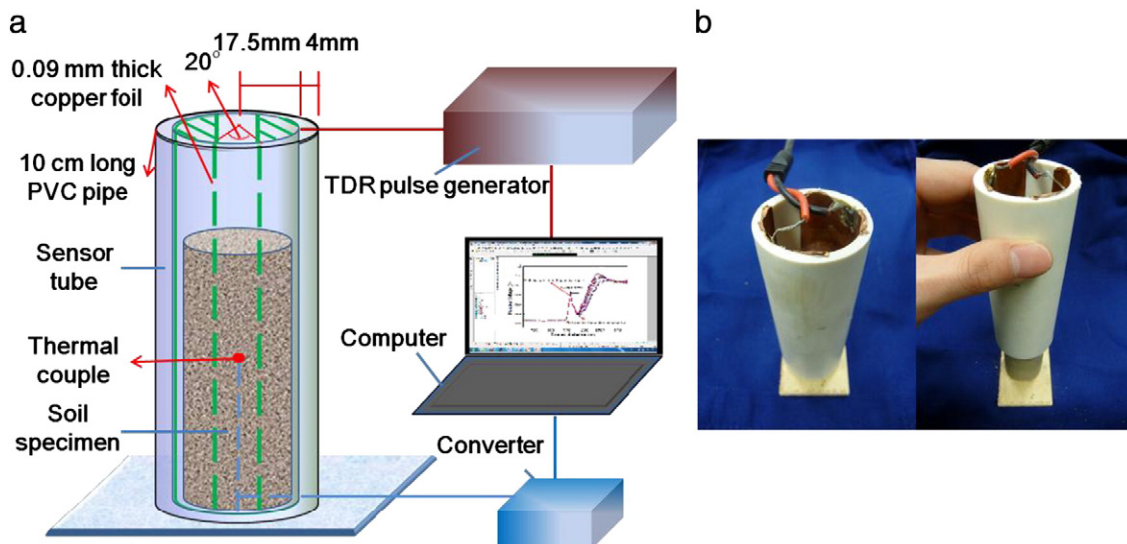


Fig. 2. a) Schematic design of TDR sensor and instrument b) TDR tube and installation.

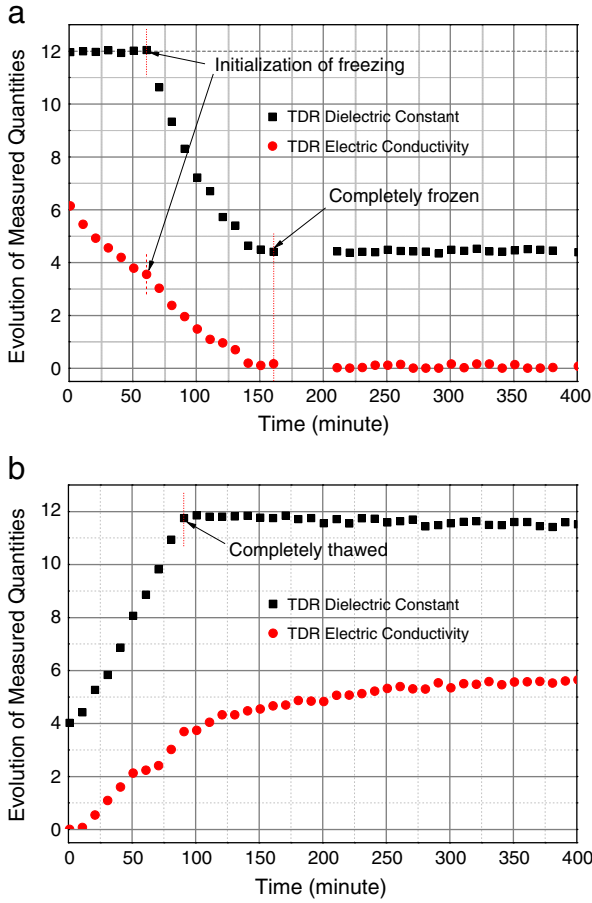


Fig. 4. Measured quantities a) in freezing process; b) in thawing process (Yu et al., 2007).

5. Sensor-assisted freeze–thaw analysis in soils

The continuum formation of the mechanical behaviours of geomaterials consists of the construction of the equation of motion, the strain–displacement correlation, and the constitutive relationship. A comprehensive mechanical model based on continuum formation was established to describe the response of soils under freezing condition. The equation of equilibrium (Eq. 12) was introduced in general tensor format in the first step.

$$\nabla \cdot (\mathbf{C} \nabla \mathbf{u}) + \mathbf{F} = 0 \quad (12)$$

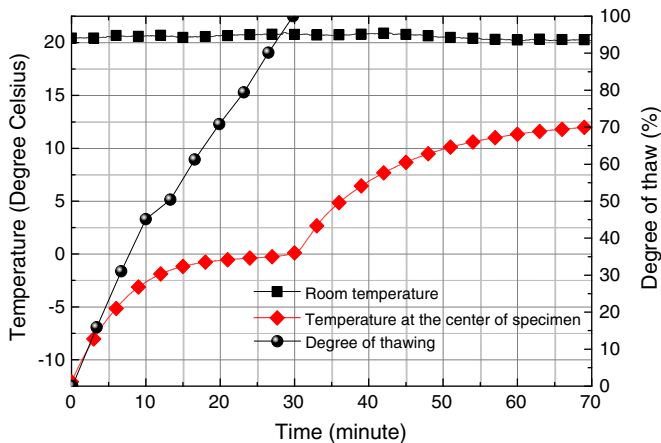


Fig. 5. Measured degree of thawing versus time.

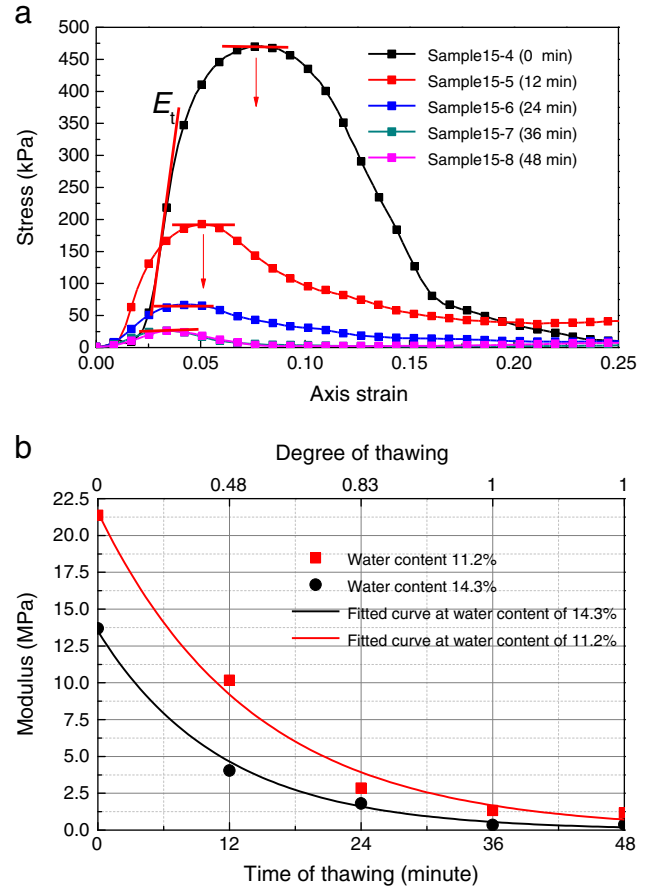


Fig. 6. a) Results of axis compression test; b) Moduli verse time and degree of thawing.

where \mathbf{u} is the displacement vector, \mathbf{C} is the fourth-order tensor of material stiffness, \mathbf{F} is the body force vector.

The strain–displacement equation is

$$\boldsymbol{\varepsilon} = \frac{1}{2} [\nabla \mathbf{u} + (\nabla \mathbf{u})^T] \quad (13)$$

The constitutive equation is

$$\boldsymbol{\sigma} = \mathbf{C} : \boldsymbol{\varepsilon} \quad (14)$$

where $\boldsymbol{\sigma}$ is the Cauchy stress tensor, $\boldsymbol{\varepsilon}$ is the infinitesimal strain tensor, the symbol “:” stands for double contraction.

In order to consider the influence of the thermal field and hydraulic field on the stress field, the constitutive relationship for porous materials was formulated by:

$$\boldsymbol{\sigma} = \mathbf{D} \boldsymbol{\varepsilon}_{el} + \boldsymbol{\sigma}_0 \quad (15)$$

where \mathbf{D} is the stiffness matrix of soil skeleton and $\boldsymbol{\sigma}_0$ is the initial stress vector, $\boldsymbol{\varepsilon}_{el}$ is the elastic strain which can be obtained from the following relationship (Liu and Yu, 2010),

$$\boldsymbol{\varepsilon} = \boldsymbol{\varepsilon}_{el} + \boldsymbol{\varepsilon}_{th} + \boldsymbol{\varepsilon}_{tr} + \boldsymbol{\varepsilon}_{\psi} + \boldsymbol{\varepsilon}_0 \quad (16)$$

where,

$\boldsymbol{\varepsilon}_{th}$ is the strain caused by thermal expansion, $[\alpha(T - T_{ref}), \alpha(T - T_{ref}), 0]^T$;
 $\boldsymbol{\varepsilon}_{tr}$ is the strain caused by the phase change of water, which was approximated by $[0.03\phi\theta_u(1 - \theta_u), 0.03\phi\theta_u(1 - \theta_u), 0]^T$ when a unit localization tensor in mixture theory is

chosen (0.09 is the relative change of volume when water turns into ice and $\theta_u = w_u \rho / (\rho_w (1 + w_u))$ is the volumetric water content at unfrozen status);

- ε_0 is the initial strain;
 ε_ψ is the strain resulting from the change of the matrix suction, which is calculated by $[-\psi \phi \theta_u / (nH), -\psi \phi \theta_u / (nH), 0]^T$.
 n is the soil porosity.

This formulation was based on the similarity between the freezing/thawing and drying/wetting process. The thermodynamics equilibrium was ensured in the multiphase porous media while plastic behavioural mechanisms were overlooked (Gary and Schrefler, 2007; Mathieu and Laloui, 2008; Pesavento et al., 2008). The strain caused by suction was derived by assuming that suction during the freezing/thawing process, ψ , can be obtained from the Clapeyron equation (Eq. 17)

$$\psi = \rho_w L_f \ln \left(\frac{T}{T_0} \right) \quad (17)$$

where ψ is the suction, L_f is the latent heat of water, T_0 is the freezing point; H is the modulus with respect to matrix suction. The value of H can be obtained by an extension of the classic theory of poroelasticity (Wang, 2000). This quantity, which is originally developed from poroelastic expansion coefficient, can be expressed by drained bulk modulus K and the Biot–Willis coefficient b as:

$$H = \frac{3K}{b} \quad (18)$$

By introducing the classical micro–macro relations of poroelasticity, Eq. (18) was transformed into

$$H = \frac{3K}{(1-K/k_s)} = \frac{EE_s}{E_s(1-2\nu) - E(1-2\nu_s)} \quad (19)$$

where k_s is the bulk modulus of soil particles, E/ν and E_s/ν_s are Young's modulus/Poisson's ratio of soil particles and of soil specimens under drained conditions, respectively.

6. Case study and practical implications

A comprehensive framework for soils under freeze/thaw effects has been established in last section. The mechanical response of a soil can therefore be readily investigated based on the freeze/thaw status identified by the TDR sensor and the corresponding mechanical properties. Detailed simulations can be carried out once initial and boundary conditions and constitutive relations are accessible. These initial and boundary conditions regarding temperature and degree of freezing/thawing can be monitored by the proposed tube sensor while the constitutive relations can be determined with conventional mechanical experiments.

This method can be further simplified for practical applications. A case study was conducted to demonstrate the application of the sensor-assisted approach to freeze/thaw analyses. A duplicate of the aforementioned soil specimen of 14.3% water content was used in this case. The soil specimen was taken out from a refrigerator at -12°C and then exposed to an ambient temperature of 22°C . The axial deformation of the specimen was monitored with a dial gauge right after the thawing process was started. The moisture loss to the environment was prevented with a piece of plastic wrap covering the whole specimens.

Since the soil specimen was only subjected to its own weight with no other lateral constraints on the top or bottom surfaces, the axial deformation was postulated to happen in a stress-free state without considering the initial stress. Due to the same reason, the axial deformation was assumed to result from the elastic strain caused by gravity, thermal expansion, and volume change due to suction and phase change of water. In view of the specimen size, the influence of gravitational

force on volume change was neglected. Then the axial strain was formulated as Eq. 20.

$$\varepsilon_L = \alpha \Delta T - 0.03 \Sigma \theta_u (1 - \theta_u) - \psi \Sigma \theta_u / (nH) \quad (20)$$

where α is 0.8×10^{-6} 1/K (Wang, 2000), ρ is the soil density which was measured to be 1.98×10^3 kg/m³, and n was assumed to be 0.7. The modulus of the freezing soil specimen was higher than that of ordinary unfrozen soil specimens. But it was still neglected since it is much smaller than that of soil grains, which varies from several GPa to more than one hundred GPa (Daphalapurkar et al., 2010).

The suction in the thawing process was conveniently calculated on the basis of Fig. 5 and Eq. (17). As can be seen, the suction decreased as the thawing process proceeded. This was because phase change of water is easier to happen in pores of big size. Therefore, smaller pores experience thawing process at a higher degree of thawing. Due to the same reason, a greater suction value corresponds to a smaller amount of meniscus and consequently smaller action area. The 0% degree of thawing was in fact not true. Based on experimental results, more than 15% of unfrozen water did still exist in the specimen at -12°C . This effect was considered in the following calculation (Fig. 7).

Plotted in Fig. 8 are the measured axial deformation and the calculated axial deformation and its components. It is seen that this simplified model succeeded in predicting the order of the magnitude of the axial deformation. Moreover, the simulated results vary similarly to the measured data. It is encouraging to predict such a complex thawing process of unsaturated soil with this simplified model. On the other hand, it is noted that there seem to be a “hysteresis” (7.5 min) between the measured and simulated data. This makes sense because the temperature used in the computation was the temperature in the center of sample. This temperature which corresponds to a greater suction value is higher than that at any other points. This error can be effectively eliminated if a comprehensive model based on physical fields rather than this simplified model is employed. In addition, it was found that suction was found to be responsible for the largest part of the deformation. Meanwhile, the deformation caused by the phase change of water did not prevail but still appreciable in the thawing process. However, the contribution from thermal expansion was negligible (Fig. 8).

7. Conclusion

This paper proposes the use of an innovative sensing method based on time domain reflectometry principles for accurate measuring the degree of freeze/thaw in soil specimens. Accordingly, traditional experiments were conducted to measure the mechanical properties of a soil during the thawing process. The combination of both types of information then enables the determination of the effects of the degree of freezing/thawing

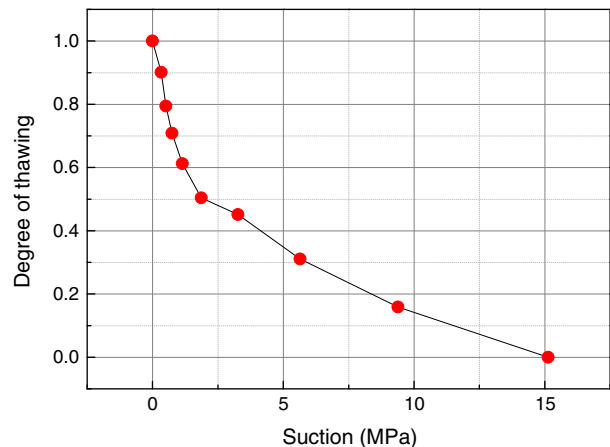


Fig. 7. Suction in freezing soils at different degree of thawing.

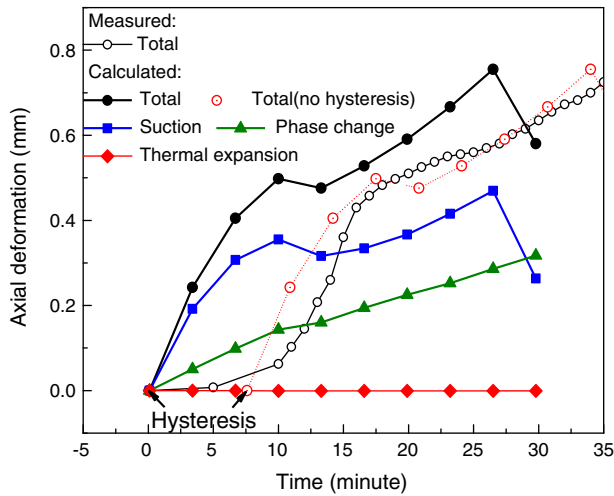


Fig. 8. Axial displacement and its components.

on the soil mechanical properties. Moreover, suction stemming from the thermodynamic equilibrium at the ice–water interface has been related to temperature which can be measured with thermocouples. A theoretical framework for freeze–thaw analysis in geomaterials was therefore established in order to utilize the aforementioned information from sensor data. This sensor-assisted analysis approach intends to serve as a holistic technique for the freeze/thaw analysis in soils and other geomaterials. A case study was presented to demonstrate the implementation of this approach. This preliminary investigation not only validated the theoretical framework but also confirmed the potential of the technique in practical applications. The technology and analysis procedures will be further refined in subsequent studies. This will not only help study the complex

soil behaviours during freeze/thaw process, but will also provide important decision-support for implementing preventative maintenance strategies for infrastructure in cold regions.

References

- Daphalapurkar, N.P., Wang, F., Fu, B., Lu, H., Komanduri, R., 2010. Determination of Mechanical Properties of Sand Grains by Nanoindentation. *Experimental Mechanics* 51 (5), 719–728.
- Drnevich, V.P., Siddiqui, S.I., Lovell, J., Yi, Q., 2001. Proceedings TDR 2001– Second International Symposium and Workshop on Time Domain Reflectometry for Innovative Geotechnical Applications. Northwestern University, Evanston, IL.
- Frost Resistivity Probe User Guide. Minnesota Department of Transportation. (1996)
- Gary, G., Schrefler, B.A., 2007. Analysis of the solid phase stress tensor in multiphase porous media. *International Journal for Numerical and Analytical Methods* 31, 541–581.
- Klut, E.A., 1986. *Methods of Soil Analysis, Part 1, Physical and Mineralogical Methods*, 2nd edition. Wiley Periodicals, Inc, Madison, Wisconsin.
- Konrad, J.M., 1994. *Canadian Geotechnical Journal* 31, 223–245.
- Liu, Z., Yu, X., 2010. *GeoFlorida 2010: Advances in Analysis, Modeling & Design*. ASCE Geotechnical Special Publication, Vol. 199, pp. 157–164.
- Mathieu, N., Laloui, L., 2008. *International Journal for Numerical and Analytical Methods* 32, 771–801.
- Neaupane, K.M., Yamabe, B., 2001. *Computers and Geotechnics* 613 Vol..
- Nishimura, S., Gens, A., Olivella, S., Jardine, R.J., 2009. *Geotechnique* 59, 159–171.
- Pesavento, E., Gawin, D., Schrefler, B.A., 2008. *Acta Mechanica* 201, 313–339.
- Roberson, R., Siekmeier, J., 2000. *Transportation Research Board*, Washington, DC, pp. 108–113.
- Siddiqui, S.I., Drnevich, V.P., 1995. Report No.: FHWA/IN/JTRP-95/9, Indiana Department of Transportation – Purdue University.
- Topp, G.C., Davis, J.L., Annan, A.P., 1980. *Water Resources Research* 16, 574–582.
- Wang, H.F., 2000. *Theory of Linear Poroelasticity with Applications to Geomechanics and Hydrogeology*. Princeton University Press, USA.
- Yu, X., Drnevich, V.P., 2004. *Journal of Geotechnical and Geoenvironmental* 130, 922.
- Yu, X.B., Liu, N., Gonzalez, J., Yu, X., 2007. Proceedings of Transportation Research Board Annual Conference.
- Yu, X., Zhang, B., Liu, N., Yu, X., 2010. *J. of Adv. Civ. Eng.* Vol. 2010. Article ID 239651, 10 pages. doi:10.1155/2010/239651.